Electronic Supporting Information for "**Chiral crystalline solids of ammonium-templated Er^{III}-formate frameworks assembled from three achiral acentric components**" by B. Liu *et al.*.

1. Synthesis.

All starting materials were commercially available, reagent grade, and used without further purification. The seven compounds were synthesized by the same method. A 10 ml of methanol and *N*,*N*-dimethylformamide (v:v = 1:1) solution containing 30 mmol formic acid and 5.0 mmol organic amine was mixed with a 5 ml of methanol solution containing 1.0 mmol $Er(NO_3)_3{\cdot}6H_2O$. The mixed solution was kept undisturbed. The crystal products were collected after several days and washed by ethanol. Formamidine was *in situ* produced from the decomposition of 1,3,5-triazine in acidic solution (see ref. 25). Yield are 40~60% based on the Er salt used. Element analysis (%): **1**, calcd. for $C_4H_8ErNO_8$: C 13.12, H 2.19, N 3.83; found: C 13.10, H 2.23, N 3.87; selected IR data (cm^{-1}): 767(m), 783 (m), 796 (m), 806 (m), 1336 (m), 1366 (s), 1371 (s), 1386 (s), 1396 (m), 1419 (m), 1469 (m), 1466 (m), 1573 (b,s), 2885(m), 2915 (m), 3080 (b,s), 3173 (s); **2**, calcd. for $C_5H_{10}ErNO_8$: C 15.83, H 2.66, N 3.69; found: C 15.86, H 2.75, N 3.68; selected IR data (cm^{-1}): 762(m), 791(m), 980(w), 999(w), 1367(sh), 1386(s), 1433(w), 1581(sh), 1631(s), 2129(vw), 2498(w), 2631(w), 2670(m), 2885(m), 2891(m), 3008(b,m), 3137(m); **3**, calcd. for $C_5H_9ErN_2O_8$: C 15.30, H 2.31, N 7.14; found: C 15.81, H 2.55, N 7.22; selected IR data (cm^{-1}): 732(m), 781(m), 796(m),1062(vw), 1123(w), 1335(m), 1351(s), 1368(s), 1385(s), 1601(s), 1707(m), 1727(m), 2737(w), 2852(m), 2954(b,w), 3329(m); **4**, calcd. for $C_5H_{10}ErN_3O_8$: C 14.74, H 2.47, N 10.31; found: C 14.71, H 2.49, N 10.40; selected IR data (cm^{-1}): 750(w), 802(m), 1013(w), 1327(m), 1368(sh), 1386(s), 1566(s), 1603(s), 1649(s), 1673(s), 2737(w), 2863(w), 2934(w), 3193(b,m), 3343(m), 3414(s); **5**, calcd. for $C_7H_9ErN_2O_8$: C 20.19, H 2.18, N 6.73; found: C 20.11, H 2.27, N 6.84; selected IR data (cm^{-1}): 637(w), 793(m), 846(w), 910(w), 983(w), 1053(w), 1102(w), 1212(w), 1321(m), 1364(sh), 1574(s), 1644(m), 2661(w), 2760(w), 2862(m), 2960(b,w), 3081(b,w), 3159(m); **6**, calcd. for $C_6H_{12}ErNO_8$: C 18.32, H 3.07, N 3.56; found: C 18.44, H 3.13, N 3.63; selected IR data (cm^{-1}): 788(m), 797(m), 1005(w), 1053(m), 1214(w), 1353(m), 1378(m), 1458(w), 1573(s), 1625(s), 1660(m), 2530(w), 2659(b,w), 2734(w), 2865(m), 2979(m), 3044(b,m); **7**, calcd. for $C_6H_{12}ErNO_9$: C 17.60, H 2.95, N 3.42; found: C 17.35, H 2.91, N 3.38; selected IR data (cm^{-1}): 795(m), 1021(w), 1071(w), 1161(w), 1281(w), 1356(m), 1376(s), 1468(w), 1519(m), 1574(s), 1642(m), 2502(w), 2669(w), 2869(w), 2935(b,m), 3025(m), 3439(m).

2. X-ray crystallography and physical measurements

The crystallographic data for the single crystals were collected at room temperature on a Nonius KappaCCD diffractometer with 2.0 kW sealed anode source using graphite monochromated Mo Kα radiation (λ = 0.71073 Å). All structures were solved by direct method and refined by full-matrix least-squares on F^2 using SHELX program. The H atoms could be located from the difference Fourier synthesis but added according to the ideal geometry. The details of data collection, data reduction and crystallographic data are summarized in Table S1, and selected molecular geometries in Table S2. CCDC-814182 to CCDC-814188 contain the supplementary crystallographic data for this paper. These data can be obtained free of charge via www.ccdc.cam.ac.uk/conts/retrieving.html (or from the Cambridge Crystallographic Data Centre, 12 Union Road, Cambridge CB2 1EZ, UK; fax: (+44) 1223-336-033; or e-mail: deposit@ccdc.cam.ac.uk).

Element analysis of carbon and hydrogen were performed on an Elementar Vario MICRO CUBE analyzer. FTIR spectra were recorded against pure samples of **1** to **7** on a NICOLET iN10 MX spectrometer in the range of 4000 to 650 cm^{-1}. Thermal analysis (TA) was performed on an SDT Q600 Simultaneous DSC-TGA Instrument at the rate of 5°C/min under air. Melting of the intermediate phases of $Er(HCOO)_3$ were observed just before the pyrolysis on a Buechi melting point B-540 instrument. Magnetic measurements were performed on Quantum Design MPMS-XL5 and MPMS-XL7 SQUID systems for polycrystalline samples tightly fixed by eicosane and sealed in capsule. Diamagnetic corrections were estimated by using Pascal constants (**1**, -99×10^{-6}; **2**, -115×10^{-6}; **3**, -126×10^{-6}; **4**, -135×10^{-6}; **5**, -139×10^{-6}; **6**, -127×10^{-6}; **7**, -138×10^{-6} cm^3mol^{-1}, respectively, and -235×10^{-6} cm^3mol^{-1} for eicosane used) and background correction by experimental measurement on sample holders. UV-vis spectra of **1** to **7** were recorded on a SHIMADZU UV-VIS-3100 spectrophotometer with an integrated sphere attachment in the range 240 – 780 nm on ground powder samples referenced to a $BaSO_4$ background.

3. Table S1 to S3

Table S1. Crystallographic Data for **1** – **7**

	1	**2**	**3**	**4**	**5**	**6**	**7**
Formula	$C_4H_8ErNO_8$	$C_5H_{10}ErNO_8$	$C_5H_9ErN_2O_8$	$C_5H_{10}ErN_3O_8$	$C_7H_9ErN_2O_8$	$C_6H_{12}ErNO_8$	$C_6H_{12}ErNO_9$
Fw	365.37	379.40	392.40	407.42	416.42	393.43	409.43
T, K	290	290	290	290	290	290	290
crystal system	monoclinic	monoclinic	orthorhombic	orthorhombic	orthorhombic	monoclinic	monoclinic
space group	$P\,2_1$	$P\,2_1$	$C\,222_1$	$P\,2_12_12_1$	$P\,2_12_12_1$	$P\,2_1$	$P\,2_1$
a, Å	6.5447(2)	6.6118(1)	6.6552(2)	6.6456(3)	6.6973(1)	6.6349(2)	6.6243(2)
b, Å	7.4781(3)	7.5662(2)	18.3549(5)	8.0898(3)	8.2497(2)	8.6371(3)	8.6345(2)
c, Å	8.7578(3)	9.2756(2)	8.4346(3)	20.155(1)	20.3822(6)	9.6727(3)	9.7545(2)
α, °	90	90	90	90	90	90	90
β, °	93.896(1)	99.827(1)	90	90	90	102.101(2)	102.599(1)
γ, °	90	90	90	90	90	90	90
V, Å^3	427.63(3)	457.22(2)	1030.33(6)	1083.56(8)	1126.13(5)	541.99(3)	544.50(3)
Z	2	2	4	4	4	2	2
D_c, g/cm^3	2.838	2.756	2.530	2.497	2.456	2.411	2.497
μ (Mo Kα), mm^{-1}	9.836	9.205	8.177	7.783	7.489	7.770	7.746
F(000)	342	358	740	772	788	374	390
Crystal size, mm^3	0.20×0.17×0.14	0.23×0.21×0.17	0.17×0.07×0.04	0.16×0.10×0.09	0.17×0.09×0.05	0.27×0.21×0.17	0.19×0.10×0.08
T_{min}, T_{max}	0.140, 0.288	0.136, 0.225	0.639, 0.726	0.354, 0.509	0.536, 0.691	0.226, 0.288	0.289, 0.614
θ_{min}, θ_{max}, °	3.59, 27.49	3.50, 27.50	4.06, 28.66	3.67, 27.41	3.64, 27.49	3.42, 27.48	3.40, 27.47
no. total reflns.	8297	8232	8267	12746	16507	9034	9594
no. uniq. reflns. (R_{int})	1959 (0.0820)	2078 (0.0602)	1330 (0.0548)	2463 (0.0792)	2592(0.0668)	2441 (0.0579)	2424 (0.0557)
no. obs. [I≥2σ(I)]	1806	1974	1177	1833	2004	2132	2211
no. params	142	139	75	155	163	148	157
$R1$, $wR2$ [I≥2σ(I)]	0.0259, 0.0532	0.0214, 0.0488	0.0224, 0.0428	0.0317, 0.0487	0.0252, 0.0476	0.0252, 0.0443	0.0204, 0.0387
$R1$, $wR2$ [all data]	0.0299, 0.0541	0.0232, 0.0492	0.0294, 0.0439	0.0585, 0.0524	0.0415, 0.0500	0.0339, 0.0455	0.0250, 0.0395
GOF	0.997	1.050	0.984	0.917	0.924	0.960	0.994
[a]Δρ, e/Å^3	1.081, −1.509	1.151, −1.109	1.002, −1.175	1.663, −1.572	0.789, −1.265	1.309, −0.736	1.150, −0.604
[b]Max. and mean Δ/σ	0.001, 0.000	0.001, 0.000	0.001, 0.000	0.001, 0.000	0.001, 0.000	0.001, 0.000	0.001, 0.000
Flack parameters	−0.06(2)	−0.04(2)	−0.01(2)	−0.03(2)	−0.03(2)	−0.02(2)	−0.05(1)

a. max and min residual density; *b*. max and mean shift/sigma.

Table S2. Selected bond distances (Å) and bond angles (°) in the Er-formate frameworks of **1** – **7**

	Er−O	O−Er−O[a]	Er−O−$C_{HCOO\ bridging}$	Er−O−$C_{HCOO\ chelating}$	C−$O_{formate}$	O−C−$O_{formate}$
1	2.318(5) ~ 2.421(5)	67.8(2) ~ 146.1(2)	125.9(5) ~ 137.6(4)	–	1.234(8) ~ 1.263(9)	123.7(14) ~ 127.1(8)
2	2.316(3) ~ 2.440(4)	68.9(1) ~ 144.1(1)	126.7(3) ~ 139.4(4)	–	1.232(8) ~ 1.271(7)	125.4(10) ~ 126.7(5)
3	2.282(3) ~ 2.399(3)	71.2(1) ~ 143.3(2)	129.8(3) ~ 149.5(6)	–	1.229(5) ~ 1.251(4)	125.1(9) ~ 126.6(6)
4	2.256(4) ~ 2.415(6)	53.9(2), 72.9(2) ~ 152.0(2)	130.9(5) ~ 148.1(4)	90.8(6 ~ 92.0(5)	1.223(9) ~ 1.286(13)	123.3(9) ~ 125.7(5)
5	2.268(3) ~ 2.578(4)	53.3(1), 71.0(2) ~ 152.1(2)	135.2(5) ~ 151.6(4)	88.1(4) ~ 97.9(4)	1.216(6) ~ 1.266(6)	121.7(6) ~ 129.4(6)
6	2.271(4) ~ 2.547(4)	52.1(1), 69.8(1) ~ 156.0(1)	135.6(7) ~ 144.1(6)	90.5(4) ~ 95.2(4)	1.180(10) ~ 1.255(7)	122.1(6) ~ 135.9(12)
7	2.258(3) ~ 2.576(3)	51.7(1), 69.8(1) ~ 157.1(1)	136.2(3) ~ 147.1(3)	90.2(3) ~ 96.0(3)	1.190(5) ~ 1.267(9)	122.0(5) ~ 134.4(5)

a. The values of 51.7(1) to 53.9(2) ° of **4** to **7** are for O−Er−O angles of chelating formates.

Table S3. The summary of static magnetic properties of **1**−**7**.

	1	**2**	**3**	**4**	**5**	**6**	**7**
C / $cm^3\ mol^{-1}$ K	11.81	11.71	11.81	11.73	12.53	12.73	12.02
θ / K	6.00	–0.12	–8.52	–11.27	–14.62	–11.49	0.93
$\chi T_{300\ K}$ / $cm^3\ mol^{-1}$ K	12.01	11.70	11.50	11.37	11.99	12.30	12.13
$\chi T_{2\ K}$ / $cm^3\ mol^{-1}$ K	10.74	7.31	4.80	5.93	6.33	6.81	10.48
$\chi T_{max.\ at\ ca.\ 18\ K}$ / $cm^3\ mol^{-1}$ K	13.70	–	–	–	–	–	12.61
$M_{50\ kOe}$ / Nβ (at 2 K)	6.29	5.85	5.69	4.79	4.68	5.13	6.30

4. Fig. S1 to S4

Fig. S1. The TGA/DSC traces for **1** to **7**: (a) TGA and (b) DSC. On DSC traces the strong endothermic peaks at ca. 310°C just before pyrolysis of the intermediate phases of $Er(HCOO)_3$ were attributed to the melting of $Er(HCOO)_3$.

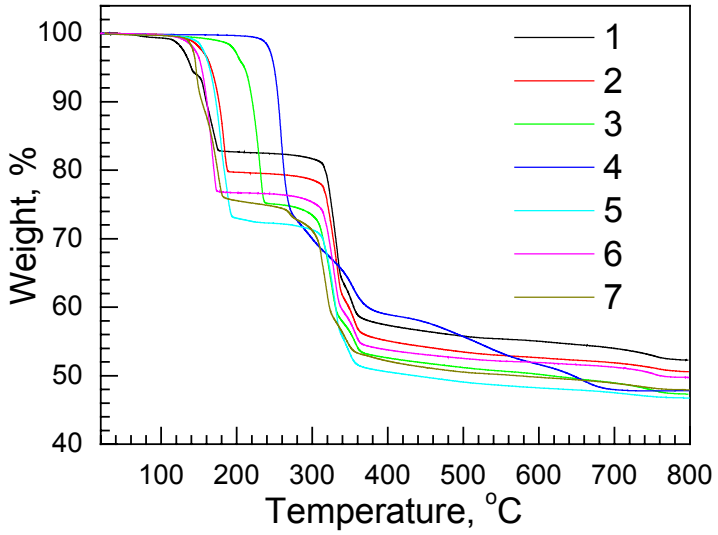

(a)

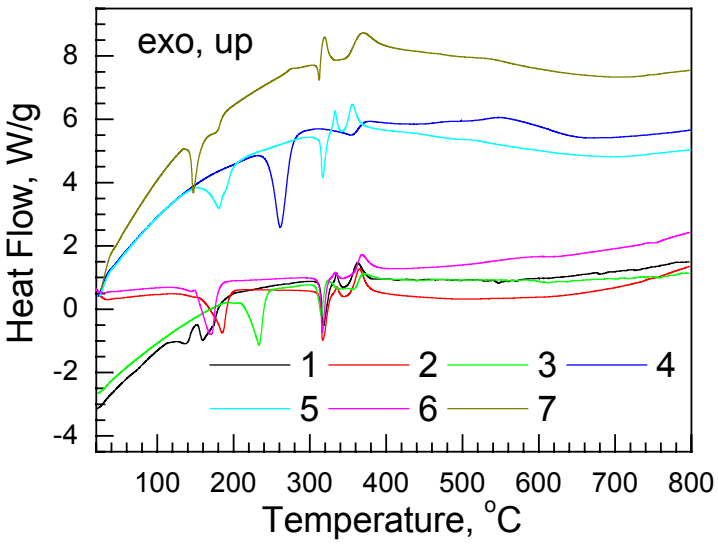

(b)

Fig. S2. The structures of **1** to **7** showing Er-formate framework and the AH^+ templates. Atomic schemes are the same as that in Fig. 1. H-atoms of formate are omitted for clarity.

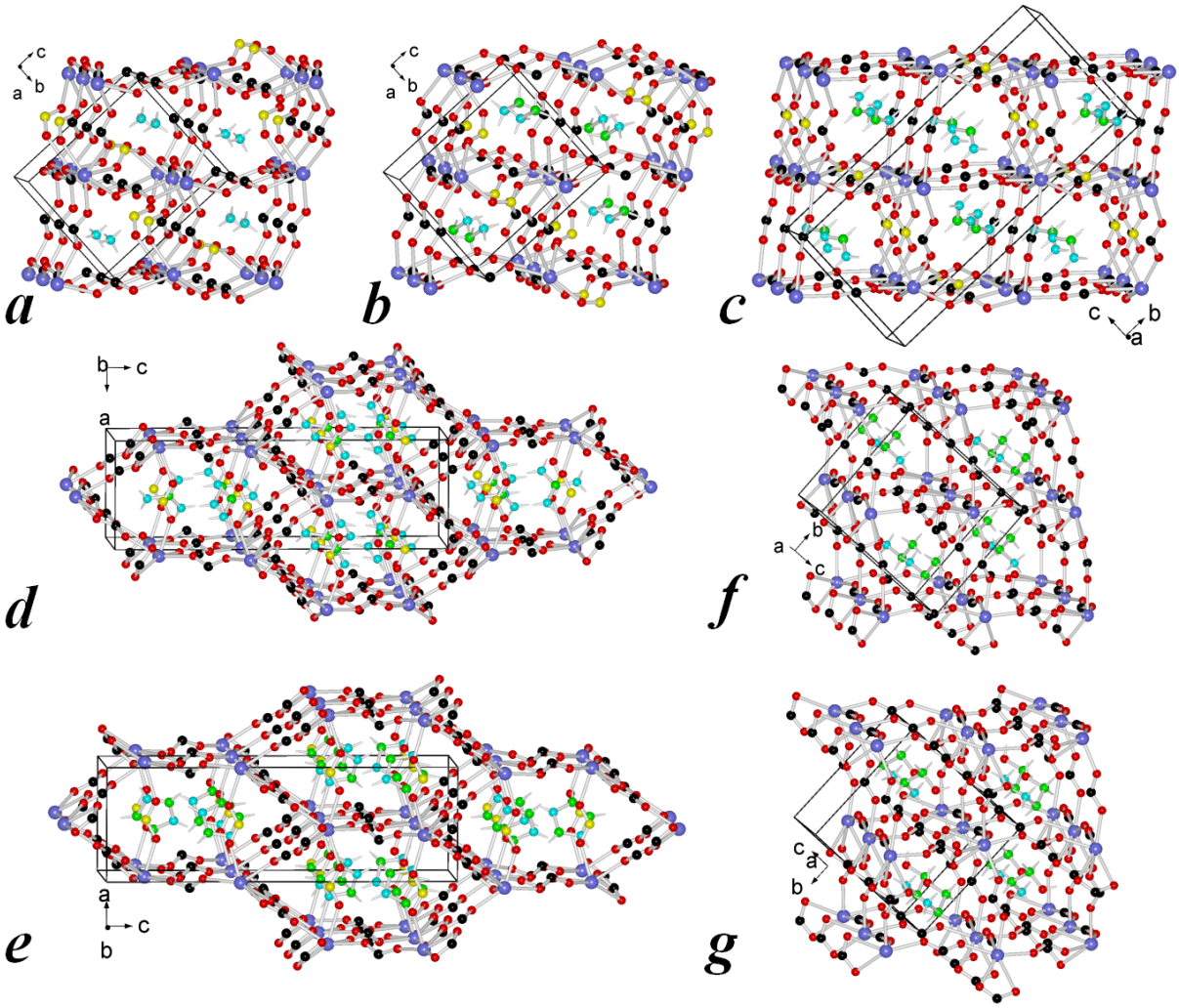

Fig. S3. The plots of framework volumes and void spaces in **1** to **7** *vs* the number of non-H atoms of AH^+ templates.

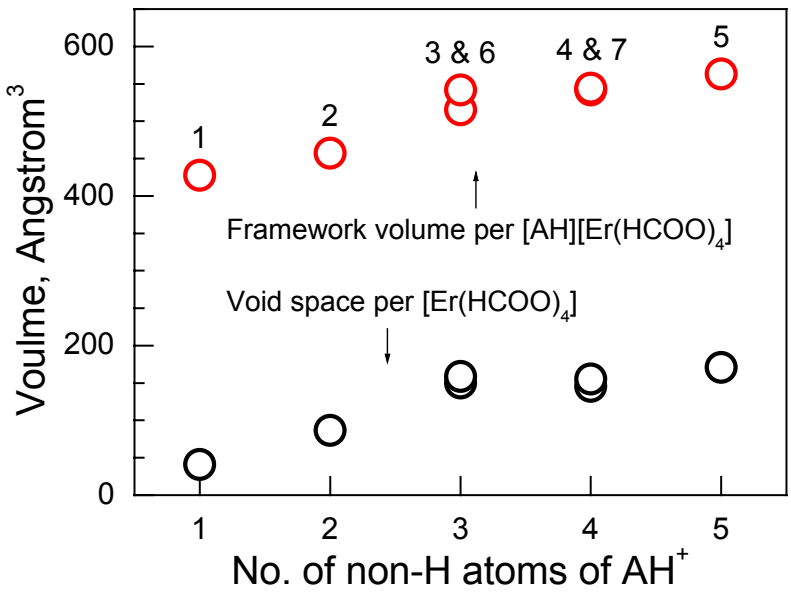

Fig. S4. The overlay of the absorption spectra of powder samples of **1** to **7**. The peak positions (in nm) and their assignments (from the ground level $^4I_{15/2}$ to the excited states). The band positions agree well with the calculated values by Judd-Oflet theory, for example, $^4I_{15/2}$ to $^4F_{9/2}$: observed 15310 cm^{-1}, calculated 15449 cm^{-1} by Judd, and $^4I_{15/2}$ to $^2H_{11/2}$: observed 19140 cm^{-1}, calculated 19407 cm^{-1}.